（23）Stress-Strain Model of Structural Members by Considering Strength Degradation (Part.1 Concrete Filled Steel Tube Members)

Yongtao BAI[1], Keita ODAWARA[2], Akihiko KAWANO[3] and Shintaro MATSUO[4]

[1]Member of AIJ, Graduate School of Human-Environment Studies, Kyushu University
(6-10-1, Hakozaki, Higashi-ku, Fukuoka, Japan)
E-mail: yongtaobai@126.com
[2]Member of AIJ, Graduate School of Human-Environment Studies, Kyushu University
(6-10-1, Hakozaki, Higashi-ku, Fukuoka, Japan)
E-mail: te106015@gmail.com
[3]Member of AIJ, Professor, Faculty of Human-Environment Studies, Kyushu University
(6-10-1, Hakozaki, Higashi-ku, Fukuoka, Japan)
E-mail: kawano@arch.kyushu-u.ac.jp
[4]Member of AIJ, Assistant Professor, Faculty of Human-Environment Studies, Kyushu University
(6-10-1, Hakozaki, Higashi-ku, Fukuoka, Japan)
E-mail: matsuo@arch.kyushu-u.ac.jp

According to the feature of inputting energy from long-period earthquakes, the risk factor by using traditional design method for high-rise buildings will be significantly increased. In order to analyze the seismic performance of super high-rise buildings under long-period ground motion, the *P-Δ* effect from vertical-loading, local buckling of steel and strain softening of concrete are essential to be overall considered. The behavior of circular and rectangular concrete filled steel tube members in high-rise building are analyzed and compared with existing tests by adopting the method of fiber-element simulation in this study. The stress-strain relationship of the confined-concrete and steel tube for circular and rectangular sections are respectively studied and proposed by considering the strength degradation after local-buckling happened. Comparison results indicate that both the pre-peak and post-peak behavior of concrete filled steel tube members in the tests can be accurately predicted by adopting the proposed model. However, the applicability of the proposed model to structural system is still needed to be investigated further.

Key Words : *Concrete filled steel tube, High-rise building, Long perod earthquake ground motions, Local-buckling, Strain softening*

1. Introduction

The design level of structures is promoted after Hyogoken-Nanbu earthquake happened in 1995, when the intensity of several observed waves are much larger than conventional design levels. Besides, oceanic severe earthquakes including Tokachi earthquake in 2003 and the 2011 off the Pacific coast of Tohoku earthquake also seriously damaged structures, especially for the long fundamental natural period strucutures under long period ground motions. Furthermore, severe Oceanic earthquakes possibly happen in Tokai, Nantokai & Nankai of Japan in the future. The seismic behavior are needed to be studied subjected to above severe earthquakes[1)].

When the super high-rise buildings under the severe ground motions stronger than assumed level, the strength deterioration of members caused by the *P-Δ* effect by vertical loadings, the local buckling of sectional steel, the buckling of main steel bar, and the concrete crush will occur. The residual deformation on single side are generated[2)], and the seismic performances of high-rise buildings rarely satisfy the seismic demand correspondingly.

Therefore, in order to investigate the seismic redundancy of high rise buildings, the *P-Δ* effect and the strength deterioration of members should be considered to elvaluate the ultimate seismic behaviors.

In this study, the stress-strain models of various elemental members in plane frame are studied, to serve as the basis of the plastic time history FEM analysis of plane frames. The strength deterioration caused by the local buckling of steel and crushing of concrete in concrete filled steel tube (CFT), steel structures (S) and reinforced concrete(RC) are considered.

In the Part. 1 of this study, the stress-strain models of steel tubular and confined concrete in square and circular CFT members are studied. The members defined by above models are verified based on the FEM analysis, by comparing with test results. The applicability of stress-strain models with considering strength deterioration is also confirmed.

2. Analythical Method

Finite element method is applied to conduct the elasto-plastic analysis. Particularly, the stiffness relationship of elements adopted in this analysis program is referred by 3), and the shear deformation is ignored. The section of beam and column elements are divided into finite tiny stress fibers, and the stress fibers are calculated based on the corresponding stress-strain relstionship models. The laws of fiber divisions for various sectional members are shown in Fig. 1~2.

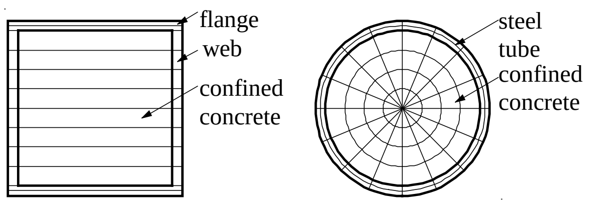

(a) Rectangular CFT (b) Circular CFT

Fig. 1 Sectional division method of fiber model

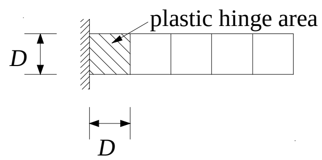

Fig. 2 Longitudinal division method of fiber model

As shown in Fig. 1, the fiber elements of rectangular section are divided along with the parallel direction of neutral axis. While, the fiber elements of circular section are divided along with the circle and radius directions simultanously.

On the longitudinal direction of column and beam members. The size of this plastic area varies with the deformation behavior after the member's plasticity. While, owing to the plastic behavior in the plastic area at the end of elements similarly distributes in this analysis program, the length of plastic area is needed to be approximated to be one certain value. Therefore, the size of plastic area is defined to be the same as the size of member's cross section along with the longitudinal direction, which is shown in Fig. 2.

3. Stress-Strain Model

In order to consider the deterioration effect of the local buckling of steel tubular and softening of confined concrete, the stress-strain models of steel tubular (square and circular) and confined concrete (in square and circular CFT members) are specifically defined and applied in the simulation of square and circular concrete filled steel tubes.

(1) Concrete Model

As shown in Fig. 3, the stress-strain model of concrete is composed of two parts, which are respectively the curve part of pre-peak and straight line part of post-peak. This type of model has been originally proposed by Park et al.[4] and Sheikh et al.[5], and it has also been applied by several researchers to be reasonable for simulation.

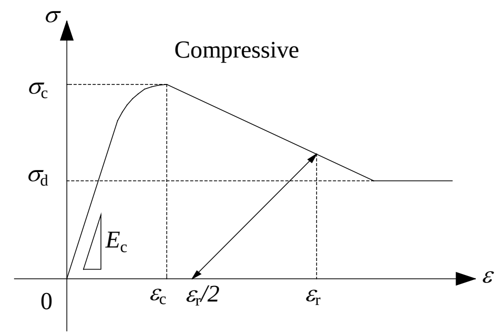

Fig.3 Stress-strain model of concrete

The constitutive relationship of confined concrete in CFT members is defined based on the model as shown in Fig. 3. In order to consider the effect of concrete softening, the model before and after compressive strength are respectively defined.

a) Model of Ascending Part

The Eq. (1) proposed by Popovics[6] is adopted to defined the stress-strain relationship before concrete achieving its compressive strength.

$$Y=\frac{VX}{1+(V-1)X^{\frac{V}{V-1}}} \tag{1}$$

$$X=\frac{\varepsilon}{\varepsilon_c}\quad,\quad Y=\frac{\sigma}{\sigma_c}\quad,\quad V=\frac{E_c\cdot\varepsilon_c}{\sigma_c}$$

Where, σ_c, ε_c is the compressive strength and the strain conrresponding to compressive strength; E_c is the Young's modulus of concrete.

b) Model of Descending Part

Besides, the stress-strain relationship after concrete achieving its compressive strength is simplified into bi-linear model. The path of unloadings and reloadings according to the law that the strain value of the intersection point of unloading line to strain axis is equal to half of the strain value (ε_r) of unloading point.

As for the confined concrete in square and circular CFT members, the formulas for defining the parameters of concrete models are different because of different confinement effect from square and circuluar steel tubulars. Similarly, owing to the different confinement effect of the concrete confined by hoop reinforcement in reinforced concrete members. The forlumae for defining the model of confined concrete in RC members are introduced in the Part. 2 of this study, which is also based on the proposal of Park et al. and Sheikh et al.

The parameters of the stress-strain model of confined concrete in CFT members are defined based on the proposal of Sakino et al.[7), 8)] based on Sargin's formula[8)] as shown in Fig. 4. The formula proposed by Sakino et al. is expressed as Eq. (2) which is drawn in Fig. 5.

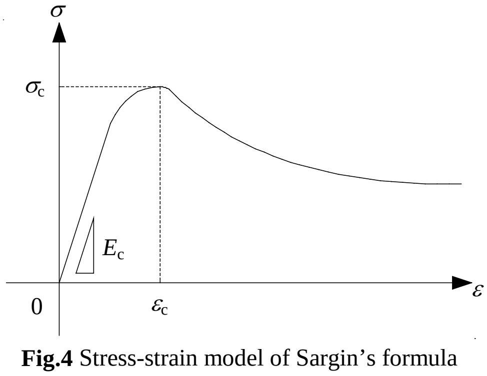

Fig.4 Stress-strain model of Sargin's formula

$$Y=\frac{VX+(W-1)X^2}{1+(V-2)X+WX^2} \tag{2}$$

$$X=\frac{\varepsilon}{\varepsilon_c}\quad,\quad Y=\frac{\sigma}{\sigma_c}\quad,\quad V=\frac{E_c\cdot\varepsilon_c}{\sigma_c}$$

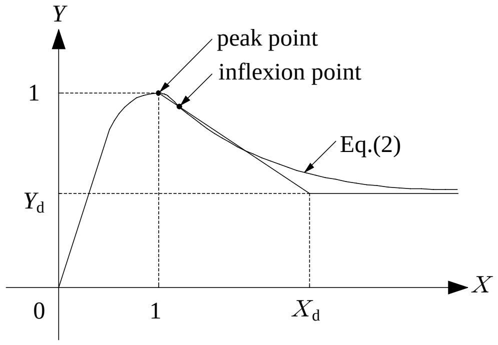

Fig.5 Bi-inear simplification of Sakino's model

In order to unify the expression and simplify the calculation, the stress deterioration model of the confined concrete in various confinement materials including hoop reinforcement, square and circular tubular are needed to be unified and proposed with the same formulas. Therefore, on the basis of Eq. (2), parameters of the confined concrete in square and circular CFT members are shown in Table 1.

As shown in Table 1, the confined strength of the concrete(σ_c) in CFT is calculated by the empirical proposal by Sakino et al. based on the test of axial loadings only on concrete part of CFT columns. The rate of strength increasement $K=\sigma_c/\sigma_p$ of the confined concrete to plain concrete is defined by considering the confinement effect from steel tubular.

Table 1 Parameters for stress-strain models for concrete

	Concrete in square CFT	Concrete in circular CFT
$\varepsilon_c/\varepsilon_p$=	1	1.0+4.7(K-1) [K≦1.5]
		3.4+20(K-1) [K>1.5]
$K=\sigma_c/\sigma_p$=	1	$1+23\sigma_{re}/\sigma_p$
σ_{re}=	$2\sigma_{wy}(B/T-1)(B/T-2)^{-3}$	$6.77\times10^{-2}\sigma_{wy}(D/T-2)^{-1}$
W=	$1.50-17.1\times10^{-3}\sigma_p+2.39\sigma_{re}^{0.5}$	

notations
- B:Outside width of steel tube [mm]
- D:Outside diameter of steel tube [mm]
- T:Thickness of steel tube wall [mm]
- E_c:Young's modulus of elasticity concrete [N/mm^2]
- σ_p:Compressive strength of plain concrete [N/mm^2]
- ε_p:Strain at maximum stress of plain concrete
- σ_c:Compressive strength of confined concrete [N/mm^2]
- ε_c:Strain at maximum stress of confined concrete
- σ_{wy}:Yield stress of steel tubular [N/mm^2]

According to Eq. (2), the stress deterioration after peak is determined by coefficient W, which is mainly depend on effective lateral restraint factor σ_{re}. The restraint factor is also affected by the shape of steel tubular (diameter thickness ratio (D/T) for circular steel tubular, width thickness ratio (B/T) for square steel tubular) and the yield strength of steel material

σ_{wy}.

For square CFT columns under low-level axial loading, the axial stress is mainly undertaken by steel tubular. Therefore, the strength improvement of confined concrete by confinement effect could be ignored compared with plain concrete, which correspond with K=1 in Table 1. Nevertheless, compared with the brittle fracture of plain concrete, the deterioration behavior of confined concrete after strength could be improved by square steel tubular. For the confined concrete in circular CFT columns, both of the strength and deterioration are improved by circular steel tubular as shown in Table 1.

Parameters of the formulae in Table 1 is based on the Sakino's proposal. In order to improve the applicability of Eq. (2), the deterioration part is needed to be simplified into bi-linear model as shown in Fig. 3.

The deterioration part of stress-strain skeleton based on Eq. (2) has an inflexion point where the curve transformed from convex curve to concave curve. bi-linear model as shown in Fig. 5 is adopted to simulate the Eq. (2) by connecting the peak point and inflexion point. As to the deterioration gradient. The bi-linear model is reasonable to simplify the model of Eq. (2).

As shown in Fig. 5, the Y_d value could be calculated by the limit value of Sargin's curve when $X\to\infty$, according to Eq. (3).

$$Y_d = \lim_{X\to\infty}\frac{VX+(W-1)X^2}{1+(V-2)X+WX^2} = 1-\frac{1}{W} \tag{3}$$

The value X_d corresponding with Y_d as shown in Fig. 4 is determined by peak point and inflexion point based on Eq. (2). Eq. (4) is proposed to define the X_d by simplified the curve of Eq. (2).

$$X_d = 1.96\left(\frac{V}{W}\right)^{0.88} + 4.77 \tag{4}$$

Eq. (4) is proposed being based on the results of multiple regression analysis, in which the V ($1 \le V \le 20$) and W ($0.5 \le W \le 5$) are adopted as the regression parameters. Finally, the proposed model as shown in Fig. 3 could be defined by the parameters calculated by Eq. (1), Eq. (3) and Eq. (4).

The compressive strength of plain concrete σ_p is reduced as 85% of the cylinder strength of concrete σ_B, which is shown as Eq. (5). The strain at maximum stress of plain concrete ε_p is defined by Popovics's proposal[6)] as shown in Eq. (6). The Eq. (7) proposed by Martines et al.[9)] is adopted to define the Young's modulus of concrete.

$$\sigma_p = 0.85\sigma_B \tag{5}$$

$$\varepsilon_p = 2.62 k_p^{0.25} \times 10^{-3} \tag{6}$$

$$E_c = \left(6.90 + 25.72\sqrt{k_p}\right)\times 10^3 \tag{7}$$

Where, k_p ($=\sigma_p/\sigma_s$) is the non-dimensional value which divide the compressive strength of plain concrete by standard strength of σ_s =60[N/mm^2]

(2) Steel Tube Model

The stress-strain skeleton model of steel tubular is shown in Fig. 6. Where, for the model before local buckling, the yielding stress-strain curve and strengthening stress-strain curve are distinctively defined by the combination of two curves of Menegotto-Pinto's hysteresis model[10)].

Further more, in order to consider the deterioration phenomenon of the square and circular steel tubular caused by local buckling in CFT members, the deterioration gradient of skeleton curve after local buckling on compressive direction is defined based on the proposal of Yamada et al.[11), 12)]. Yamada et al. has studied the modeling of the stress-strain model to predict the ultimate behavior of hollow square steel tubular and H-shaped steel subjected to compression loadings based on the test results of short columns. According to the proposal of Yamada et al., deterioration part of stress-strain relationship is affected by production methods and material properties, therefore, it is also recommended to simplify the deterioration behavior into bi-linear curves.

The details of the skeleton curve and hysteresis model of stress-strain relationship are introduced in the part. 2 of this study. Parameters of ε_m, r_d, τ_{d1}, τ_{d2} for defining the deterioration model of the square and circular steel tubular in CFT members is shown in Fig. 6. The formulas of above parameters for steel tubular in CFT members are the same as the formulae for defining the hollow steel tubular in the part. 2 of this study. The behavior of the local buckling and post local buckling of steel tubular is also affected by confined concrete in steel tubular.

a) Steel Tubular in Square CFT

When the local buckling of CFT column happens under low axial loadings, the axial loadings are mainly taken by steel tubular, and the effect of the volume expansion of confined concrete could be ignored simultanously.

Specifically for square CFT columns, although the volume expansion of confined concrete could be ignored when CFT columns under the low level of axial loadings, the confinement effect of the concrete on the interior instability of steel tubular is still be considered.

Thus, in order to consider the confinement of the concrete to interior steel tubular compared with hollow steel tubular. The strain ε_{m} of steel model for CFT members when local buckling happening is proposed to be increased than that of hollow steel tubular.

ε_{m} is calculated according to the formula based on the proposal of Kawano[13)], which is expressed as Eq. (8). Eq. (8) is proposed by modified from the corresponding formula of hollow steel tubular as shown in the Part. 2 of this study.

$$\varepsilon_{\mathrm{m}} = \left[13.5 \left\{ \left(\frac{B}{T} \right)^2 \cdot \varepsilon_{\mathrm{y}} \right\}^{-1.4} + 1 \right] \cdot \varepsilon_{\mathrm{y}} \tag{8}$$

Where, B is the width of square steel tubular, T is the thickness of square steel tubular. Further, Suzuki et al.[14)] proposed that the local buckling behavior of the square steel tubular with certain B/T is mainly equal to that of square CFT columns with 1.32×B/T. Therefore, the Eq. (9) for calculating the factors of r_{d}, τ_{d1} is modified as 1/1.32 times to that of hollow steel tubular which is introduced in the Part. 2 of this study.

$$\begin{aligned} \alpha &= \left(\frac{1}{1.32} \cdot \frac{B}{T} \right)^2 \cdot \varepsilon_{\mathrm{y}} \\ r_{\mathrm{d}} &= -0.079\alpha + 0.81 \\ \tau_{\mathrm{d1}} &= -0.014\alpha^2 - 0.005 \end{aligned} \tag{9}$$

Where, α is the standardization ratio of width to thickness ratio; τ_{d1} is the rate of the buckling negative slope to Young's modulus; r_{d} is the rate of the post-buckling strength to the buckling strength.

As to the deterioration gradient of post-buckling, the interaction confinement between concrete and steel tubular starts to work when the deformation of CFT columns grows after local buckling happened. The strength of steel tubular shows stable behavior based on the observations of previous test results[15)], thus, the deterioration gradient $\tau_{\mathrm{d2}} \cdot E_{\mathrm{s}}$ of post-buckling is empirically determined as 0.

Therefore, the rate of the post-buckling degative slope to Young's modulus τ_{d2} is calculated by Eq. (10).

$$\tau_{\mathrm{d2}} = 0 \tag{10}$$

Where, τ_{d2} is the rate of the post-buckling negative slope to Young's modulus.

Ultimately, the deterioration behavior of the stress-strain model of square steel tubular is defined based on the Eq. (8), Eq. (9) and Eq. (10), which is the function of B/T and ε_{y}.

b) Steel Tubular in Circular CFT

As to circular CFT column members, the exterior deformation of steel tubular grows larger than the expansion of confined concrete under the low level of axial loading, as a result, there is no contact between the confined concrete and circular steel tubular. Thus, the buckling behavior of circular steel tubular in CFT members is the same as that of hollow steel tubular.

The Eq. (11) of ε_{m} for circular hollow steel tubular introduced in the Part. 2 of this study is adopted as that of the circular steel tubular in CFT members, based on the modification of Kawano's proposal[13)].

$$\varepsilon_{\mathrm{m}} = \left\{ 0.18 \cdot \left(\frac{D}{T} \cdot \varepsilon_{\mathrm{y}} \right)^{-1.4} + 1 \right\} \cdot \varepsilon_{\mathrm{y}} \tag{11}$$

Where, D (mm) is the diameter of steel tubular; T (mm) is the thickness of steel tube; r_{d} is the is rate of the post-buckling strength to the buckling strength; τ_{d1} is the rate of buckling negative slope to Young's modulus. r_{d} and τ_{d1} are calculated by Eq. (12), which is introduced in the Part. 2 of this study in detail. The Eq. (12) is proposed on the basis of the stress degradation theory caused by local buckling proposed by Ochi et al.[16)].

$$\begin{aligned} r_{\mathrm{d}} &= 3.37 \left(\frac{D}{T} \cdot \varepsilon_{\mathrm{y}} \right)^{-0.07} - 3.576 \\ \tau_{\mathrm{d1}} &= -0.12 \left(\frac{D}{T} \cdot \varepsilon_{\mathrm{y}} \right)^{0.48} + 0.011 \end{aligned} \tag{12}$$

The post-buckling deterioration of circular steel tubular is considered to be the same as that of square steel tubular. The rate of post-buckling negative slope to Young's modulus τ_{d2} is also fixed as 0 based on the Eq. (10), because of the confinement effect

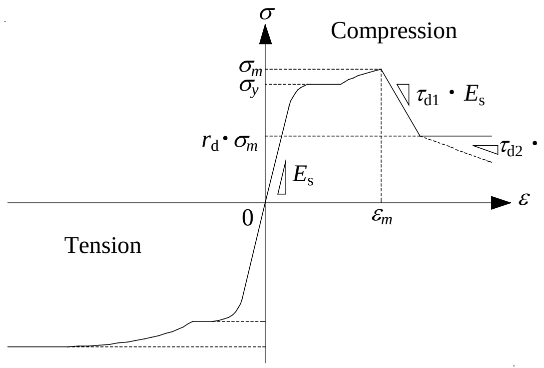

Fig.6 Skeleton curve of steel material

between concrete and steel tubular along with the increasing of lateral deformation.

Therefore, the deterioration model of stress-strain relationship could be defined by Eq. (10), Eq. (11) and Eq. (12) which are respectively the function of the diameter thickness ratio (D/T) and yield strain of steel (ε_y) material.

4. Model Verification

The simulations of several test specimens are conducted to verify the accuracy of the stress-strain models of confined concrete and steel tubular mentions in the chapter 3 of this paper. The loading procedures include horizontal cyclic loading with vertical constant and central loading as shown in Fig. 7.

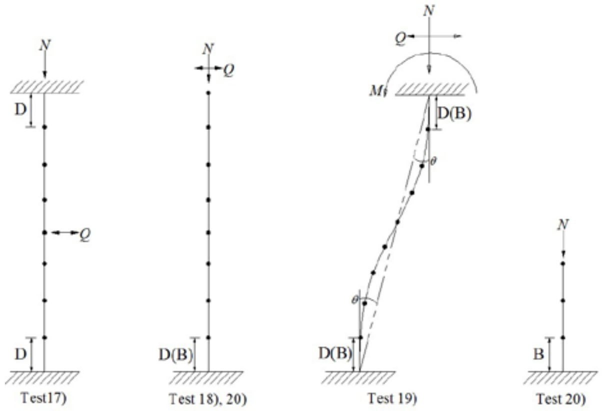

Fig. 7 Loading procedures of test simulation

(1) Circular CFT columns

The stress-strain models of Confined concrete and steel tubular are applied to simulate the seismic behavior of the circular CFT beam-columns, which is referred from the experimental studies of circular CFT columns subject to cyclic loadings with vertical constant loadings conducted by A. Elremaily et al.[17], Yan Xiao et al.[18] and Eiichi. Inai et al.[19], the parameters of each test specimens are shown in Table 2.

The comparisons of the hysteresis curves between test results and analytical results are shown in Fig. 8~10. Furthermore, in order to investigate the accuracy of simulations, three factors of *F-D* relationship are selected and analyzed, which are respectively the strength, deformation at strength and deterioration gradient after strength. Three factors mentioned above are calculated and compared between test and analysis, the rate of test results to analysis results are are shown in Fig. 11.

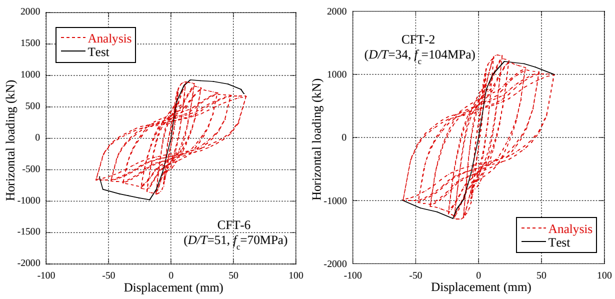

(a) D/T=51 (b) D/T=34

Fig. 8 Comparisons of hysteresis hoops between test[17] and analysis results

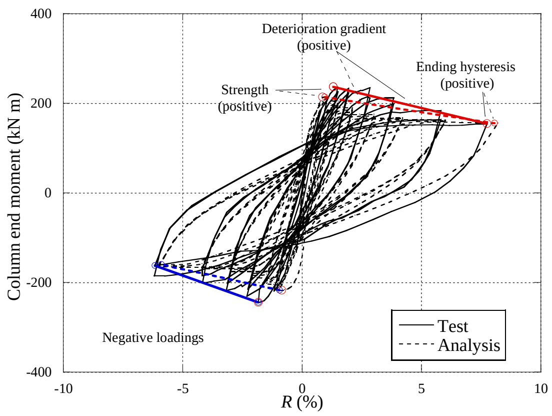

Fig. 9 Comparisons of hysteresis hoops between test[18] and analysis results

Table 2 Matrix of the circular CFT test specimens

References	Specimens NO.	Geometrical properties				Material properties		Axial load level
		D/T	T(mm)	D	L (mm)	f_c (MPa)	σ_y (MPa)	N/N_0
A. Elremaily et al.[17]	CFT-1	51	6.4	326.4	914	100	372	0.33
	CFT-5	51	6.4	326.4		40		0.4
	CFT-6	51	6.4	326.4		70		0.32
	CFT-2	34	9.5	323		104		0.2
	CFT-3	34	9.5	323		104		0.4
	CFT-4	34	9.5	323		40		0.42
Yan Xiao et al.[18]	C1-CFT3	112	3	336	1500	39.1	303	0.47
Eiichi. Inai et al.[19]	SC4-A-4-C	53	4.5	240	1440	40	276	0.4
	SC4-A-9-C	53	4.5	240		90	276	0.4

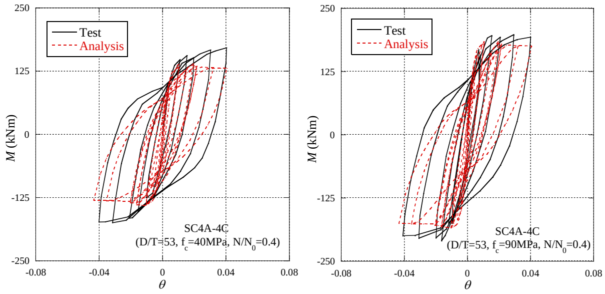

(a) SC4-A-4C (b) SC4-A-9C

Fig. 10 Comparison of hysteresis hoops between test[19] and analysis results

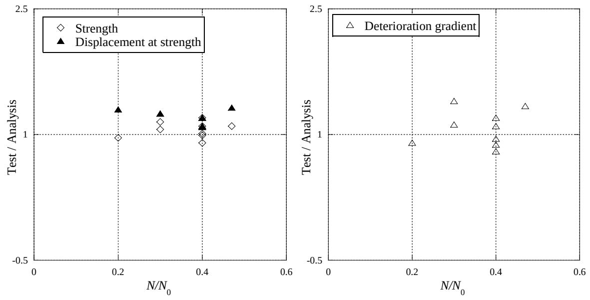

Fig. 11 Accuracy verification based on three factors

As shown in Fig. 8~10, it is intergrally observed that the analytical hysteresis curves could accurately predict the behavior of the test results with reasonable underestimation. The error between analytical results and test results may caused by the operations in experiment, constitutive models and the calculation method.

According to the comparison of the strength capacity, Displacement at strength and deterioration which are averaged on both positive and negative directions. It could be observed from Fig. 11 that test results are underestimated by simulations globally, and the rate of differentials are mainly forced among 0.9~1.25. In particular, the deterioration gradient always keeps around 1.0, which means that the post-buckling deterioration could be predicted with good correlation.

(2) Square CFT columns

Similarly, the accuracy of the concrete and steel tubular models proposed in this article is also needed to be verified. References[20)~22)] of experimental studies of square CFT specimens subjected to cyclic loadings and axial loadings are analyzed, and the representative comparisons are conducted and shown in Fig. 12~13.

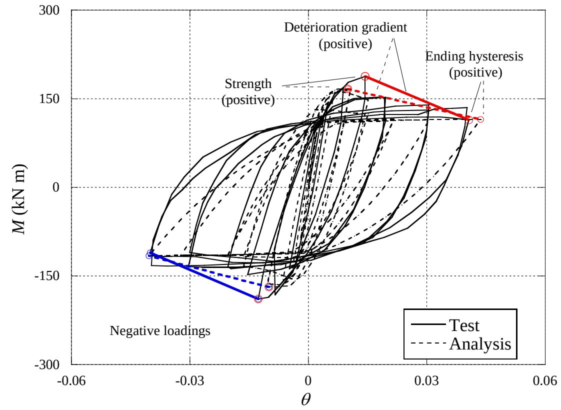

(a) SR4-A-4-C[19]

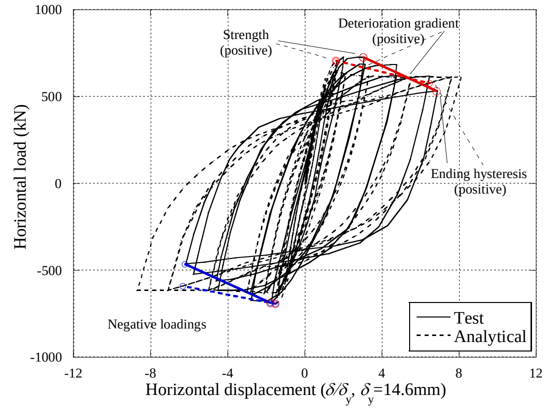

(b) CBC-32-80-10[20]

Fig. 12 Comparison of hysteresis hoops between test and analysis results

Table 4 Matrix of square CFT test specimens

Authors	Specimen	f_y	f'_c	B/T	T (mm)	L (m)	N/N_0
E. Inai et al.[19]	SR4-A-4-C	295	35.5~42.4	35	6.0	1.26	0.4
	SR4-A-9-C	295	84.5~94.5	35	6.0	1.26	0.4
	SR4-C-4-C	276	35.5~42.4	47	4.5	1.26	0.4
	SR4-C-9-C	276	84.5~94.5	47	4.5	1.26	0.4
Varma, Ricles et al.[20]	CBC-32-80-10	600	110	32	8.9	1.5	0.1
	CBC-32-80-20	600	110	32	8.9	1.5	0.2
	CBC-48-80-10	660	110	48	6.1	1.5	0.11
	CBC-48-80-20	660	110	48	6.1	1.5	0.22
L.-H. Han[21]	r1-1	228	48.3	35	2.86	0.3	
	r2-1	228	48.3	42	2.86	0.36	

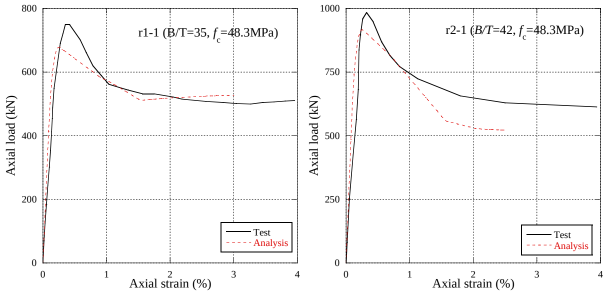

(a) r1-1 (b) r2-1

Fig. 13 Comparison of axial strength & strain curves between test[22] and analysis results

The strength of specimens is reasonably underestimated by analysis program as shown in Fig. 12, the deterioration are accordingly affected by the strength underestimation. Meanwhile, the peak-point of every hysteresis curves of test and analytical results approaches after strength achieved, and ultimately, the envelope curves of test and analysis degrade in the similar direction. Comparisons of the specimens under axial compressive loading are shown in Fig. 13, the strength and degradation of square CFT members under monotonic axial compression could be well predicted.

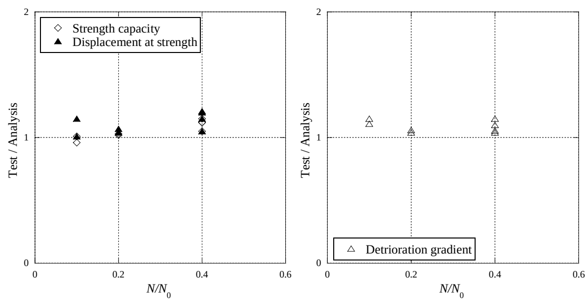

Fig. 14 Accuracy verification based on three factors

Furthermore, in order to verify the accuracy of concrete and steel models, strength, displacement at strength and deterioration are also calculated and compared between test and analytical results as shown in Fig. 14. From Fig. 14, it shows good agreement between test and prediction, while, the analytical deterioration gradient (negative value) is slightly larger than that of test. This phenomenon is because that the underestimation strength decreases the gradient of negative slope.

CONCLUSIONS

For CFT members, the stress-strain models of confined concrete and steel tubular (square & circular hollow section) by considering local buckling and deterioration are developed. Certain amount of square and circular CFT columns are simulated on the basis of

1) The stress-strain models of confined concrete in square and circular CFT members are respectively developed being based on the Popovis's proposal for ascending relationship and Sargin & Sakino et al.' proposal for descending relationship.

2) in order to consider the effects of local-buckling and deterioration, the stress-strain models of square and circular steel tubular in CFT members are proposed by being modified from that of the hollow steel tubular based on regression analysis.

3) Several experimental studies of square and circular CFT members are simulated. According to the comparison results, the seismic behavior of CFT members under cyclic loading could be accurately predicted by adopting the material models developed in this article with slight underestimation.

(4) The consideration of deterioration effect is necessary, and the stress-strain models of concrete and steel tubular in CFT members is applicable for analyzing the CFT high-rise buildings, further.

ACKNOWLEDGEMENTS

This study was financially supported by the Grants-in-Aid for Scientific Research (B) No.20360254 (Principal Investigator: Professor Uetani). The assistance on the content of this paper provided by Professor Uetani and A. professor Araki is gratefully acknowledged.

REFERENCES

1) Building Rearch Institute: Study on the Safety Countermeasures for Super-High-Rise Buildings etc. against the Long-Period Earthquake Ground Motions, December, 2010.
2) Y.M. Kim, M. Araki, Yamakawa, H. Tagawa, K. Ikago: Influence of D-Delta Effect on Dynamic Response of High-rise Moment-Resisting Steel Building Dubject to Extreme Earthquake Ground Motions, *Journal of Structural and Constructional Engineering*, No. 644, pp. 1861-1868, 2009.
3) A. Kawano and R.F. Warner: Nonlinear Analysis of the Time-Dependent Behaviour of Reinforced Concrete Frames, *Research Report No. R125*, Department of Civil and Environmental Engineering, The University of Adelaide, 1995.
4) D. Kent & R. Park,: Flexural Members with Confined Concrete, *Proceedings* ASCE, Vol. 97, ST7, pp. 1969-90, 1971.
5) S.A. Sheikh and S.M. Uzumeri: Analytical model for concrete confinement in tied columns, *Journal of Structural Engineering*, ASCE, Vol. 108, pp.2703-2722, 1982.
6) S. Popovics: A Numerical Approach to Complete Stress-Strain Curve of Concrete, Cement and Concrete Research, pp. 583-599, 1973.
7) Kenji Sakino, Yuping Sun: Stress-Strain Curve of Concrete Confined by Rectilinear Hoop, *Journal of Structural and Constructional Engineering*, No. 461, pp. 95-104, 1994.
8) K. Sakino, H. Nakahara, S. Morino and I. Nishiyama: Behavior of Centrally Loaded Concrete-Filled Steel-Tube Short Columns, *Journal of Structural Engineering*, ASCE, Vol. 130, pp. 180-188, 2004.
9) S. Martinez, A.H. Nilson and F.O. Slate: Spirally Reinforced High-Strength Concrete Columns, *ACI Journal*, Vol. 81, No.

35, pp. 431-442, 1984.
10) M. Menegotto and P.E. Pinto: Method of Analysis for Cyclically Loaded RC Frames Including Changes in Geometry and Non-Elastic Behavior of Elements under Combined Normal Force and Bending, *IABSE Congress Reports of the Working Commission Band*, No. 13, 1973.
11) S. Yamada, H. Akiyama and H. Kuwanura: Deteriorating Behavior of Wide Flange Section Steel Members in Post Buckling Range, *Journal of Structural and Constructional Engineering*, No. 454, pp. 179-186, 1993.
12) S. Yamada, H. Akiyama and H. Kuwanura: Post-Buckling and Deteriorating Behavior of Box-Section Steel Members, *Journal of Structural and Constructional Engineering*, No. 444, pp. 135-144, 1993.
13) A. Kawano: A Criteria for Local Buckling of Concrete Filled Tubular Members Under Cyclically Repeated Loading, *Journal of Structural and Constructional Engineering*, No. 608, pp. 151-156, 2006.
14) T. Suzuki, S. Motoyui and H. Ohta. Buckling and Post Buckling Behavior of Concrete Filled Rectangular Steel Tubular Stub Columns Under Pure Axial Compression, *Journal of Structural and Constructional Engineering*, No. 486, pp. 143-151, 1996.
15) H. Nakahara, K. Sakino and E. Inai: Analytical Model for Axial Compressive Behavior of Concrete Filled Square Steel Tubular Columns, Japan Concrete Institute, No. 20, pp. 817-822 , 1998.
16) K. Ochi and Y. Kurobane: Statistical Evaluation of Load-Carrying and Deformation Capacities of Cold-Formed Circular Tubular Members, *Journal of Structural and Constructional Engineering*, No. 391, pp. 59-71, 1988.
17) A. Elremaily, A. Azizinamini: Behavior and strength of circular concrete-filled tube columns, *Journal of Constructional Steel Research*, No. 58, pp. 1567-91, 2002.
18) Y. Xiao, W. He, Kang-kyu Choi: Confined Concrete-Filled Tubular Columns, *Journal of Structural Engineering*, Vol. 131, No. 3, pp. 488-197, 2005.
19) Eiichi. Inai, A. Mukai, M. Kai, H. Tokinoya, Toshiyuki Fukumoto and Koji Mori: Behavior of Concrete-Filled Steel Tube Beam Columns, *Journal of Structural Engineering*, Vol. 130, No. 2, pp. 189-202, 2004.
20) A.H. Varma, James M. Ricles, Richard Sause, Le-Wu Lu: Seismic Behavior and Design of High-Strength Square Concrete-Filled Steel Tube Beam Columns, *Journal of Structural Engineering*, Vol. 130, No. 2, pp. 169-179, 2004.
21) L.H. Han: Tests on stub columns of concrete-filled RHS sections. *Journal of Construction Steel Research*, No. 58, pp. 353-372, 2002.